Modeling, Simulation and Experimental Validation of a DC Power System Testbed

M. Bash, R. R. Chan, J. Crider, C. Harianto, J. Lian, J. Neely, S. D. Pekarek, H. Suryanarayana, S. D. Sudhoff and N. Vaks
School of Electrical and Computer Engineering
Purdue University, West Lafayette, IN 47907-2035, USA sudhoff@ecn.purdue.edu

Y. Lee, E. Zivi
Weapons & Systems Engineering Department
United States Naval Academy
Annapolis, MD 21403, USA
zivi@usna.edu

Keywords: DC, power system, detailed waveform, average value, stability

Abstract

The modeling, simulation and experimental validation of the primary bus components of a dc power system testbed are presented herein. This reduced scale and reduced complexity dc testbed is representative of medium voltage dc (MVDC) systems being considered for shipboard next generation integrated power systems (NGIPS). The primary system components include a 4-pole wound-rotor synchronous generator and a propulsion drive based on an induction machine driven by a fully controlled three-phase bridge inverter with an input filter. Four simulation models are presented: a detailed waveform model, a simplified waveform model, a detailed non-linear average value model, and a simplified non-linear average value model. These models have been implemented in the Advanced Continuous Simulation Language (ACSL). The simplified waveform and average value model (AVM) versions of the ACSL truth models were converted to Simulink to aid dissemination to other researchers. System stability is addressed via time domain simulation and a generalized immittance based stability analysis. The time-domain models and frequency domain stability analysis provide consistent results validated by the experimental results provided herein.

1. TESTBED OVERVIEW

The dc testbed reflects the U.S. Navy's interest in medium voltage dc systems for future ships. This testbed is located at Purdue University and is one of several Office of Naval Research (ONR) sponsored Electric Ship Research and Development Consortium (ESRDC) integrated simulation / stimulation (SIM/STIM) testbeds. Work is also currently underway to establish geographically distributed SIM/STIM capabilities with other ESRDC laboratory facilities. ESRDC is composed of Florida State University, Mississippi State University, MIT, the Naval Postgraduate School, Purdue University, University of South Carolina, University of Texas-Austin and the U.S. Naval Academy. More information about ESRDC can be obtained from www.ESRDC.com and reference [1].

As shown in Figure 1, the dc testbed subset primary bus components included in this study are:

1. Generation system 1 (GS-1) 59 kW wound rotor synchronous machine with Voltage Regulator-1 (VR-1) and passive Rectifier R-1 driven by a four-quadrant dynamometer prime mover emulator.
2. Ship propulsion system (SPS) a 37 kW induction machine (IM) connected to a dynamometer hydrodynamic load emulator.

Reports, models, parameter data, simulations and experimental results are available for download at www.usna.edu/ESRDC.

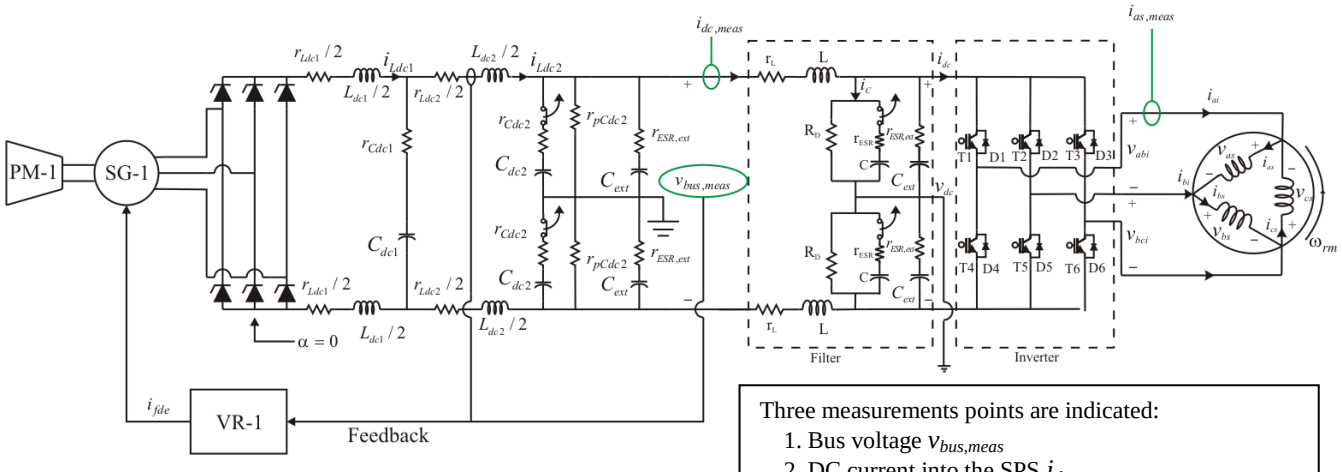

Figure 1 DC testbed primary bus components

Additional dc testbed components not presented in this study include:

3. Generation system 2 (GS-2) 11 kW permanent magnet synchronous machine with voltage regulator-2 (VR-2) and an inverter serving as rectifier R-2 driven by a four-quadrant dynamometer prime mover emulator.
4. Power supply 1 (PS-1) which steps down the 750 V primary dc bus to the 500 V port-side dc distribution bus.
5. Power supply 2 (PS-2) which feeds the 500 V starboard-side dc distribution fed by a 480 VAC utility grid connection.
6. Three dc distribution zones which include: switchgear, conversion modules, inverter modules and load banks.
7. One pulsed power load (PPL) is designed to place a load on the testbed which is representative of a pulsed power weapon such as a radar or rail gun.

Reference [2] provides a comprehensive description of the dc tested including detailed models, parameter values and preliminary test results. The test results included herein supersede the preliminary test results in the reference.

The dc testbed is an extension of prior U.S. Navy funded research which included the establishment of a Naval Combat Survivability (NCS) Testbed [3]. The NCS testbed contained an ac primary distribution bus feeding the propulsion load as well as redundant port and starboard dc zonal distribution buses, converters, switchgear and loads. Research under this prior effort included the development of advanced stability analysis tools, power converter control strategies, new time-domain simulation tools, improvement in multi-level power conversion and electric drive propulsion, advanced methods of parameter identification, and investigations into the system effects of pulsed power loading [4].

2. GENERATOR MODEL

As shown in Figure 3, the GS-1 generation system consists of the PM-1 prime mover emulator, a SG-1 synchronous generator, a VR-1 voltage regulator, a R-1 line commutated rectifier, a brushless exciter and an output low-pass filter. The synchronous generator is a 4-pole wound-rotor synchronous machine which is rated to supply 59 kW at 1800 rpm. The output of the generator is rectified by a three phase line commutated diode rectifier. The brushless exciter and VR-1 PI voltage regulator provides a 750 V nominal bus voltage. The low-pass LC output filter helps prevent high frequency components, mainly from switching, from propagating on to the dc bus.

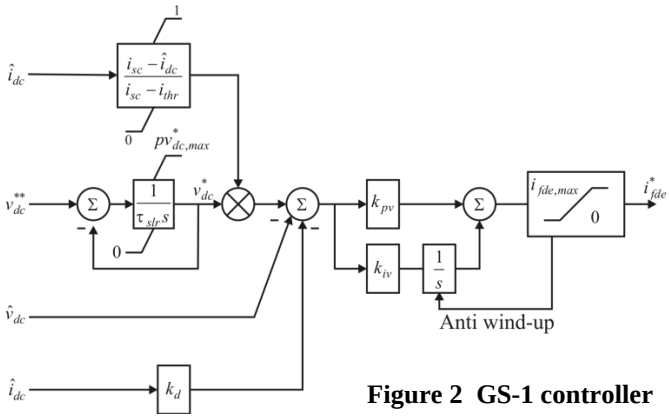

Figure 2 GS-1 controller

The one-line diagram of the GS-1 controller is depicted in Figure 2. Therein, v_{dc}^{**} denotes the reference (or commanded) dc voltage, $\hat{v}_{dc}$ denotes the low-pass filtered dc bus voltage with filter time constant τ_{fv}, and $\hat{i}_{dc}$ denotes the low-pass filtered inductor current with filter time constant τ_{fi}. The reference dc voltage is slew-rate limited to prevent excessive capacitor inrush currents on startup. Short circuit protection is also included by sharply reducing the voltage command when the current exceeds a certain threshold. The droop term, k_d, allows multiple generators to share the load. Voltage regulation utilizes a PI control with anti wind-up. The output of the controller is the commanded field current into the brushless exciter, i_{fde}^{*}.

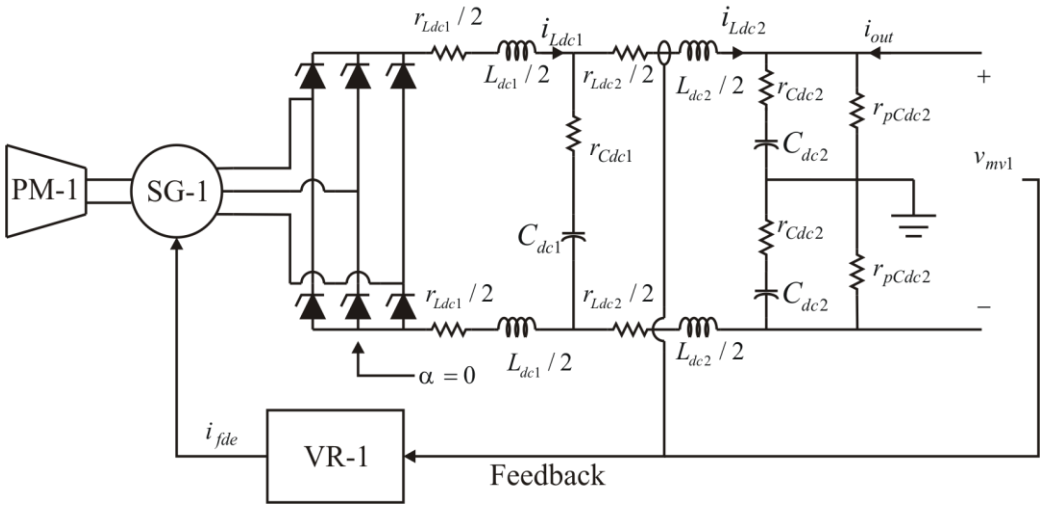

Figure 3 Generation source GS-1

The detailed GS-1 model employs a transfer function model [5], [6] in place of the equivalent circuit model commonly found in the literature. The simplified synchronous machine model uses conventional modeling techniques [7] set forth in [8]. The simplified brushless exciter model uses a transfer function representation. The lumped parameters required for the simplified synchronous machine are obtained by curve fitting the frequency response of the machine to the *q*- and *d*-axis transfer functions [5]. The nonlinear AVM models are more suitable for control design and dynamic response studies of complex dynamically interdependent systems [9]. The average value model of GS-1 uses a reduced order model of the synchronous machine which neglects the stator dynamics; more detail is presented in [7]. The average value model of the rectifier is set forth in [8]. The other aspects of the GS-1 AVM model are similar to the detailed waveform model. Complete models, parameter data, and simulations can be obtained from reference [10] or www.usna.edu/ESRDC.

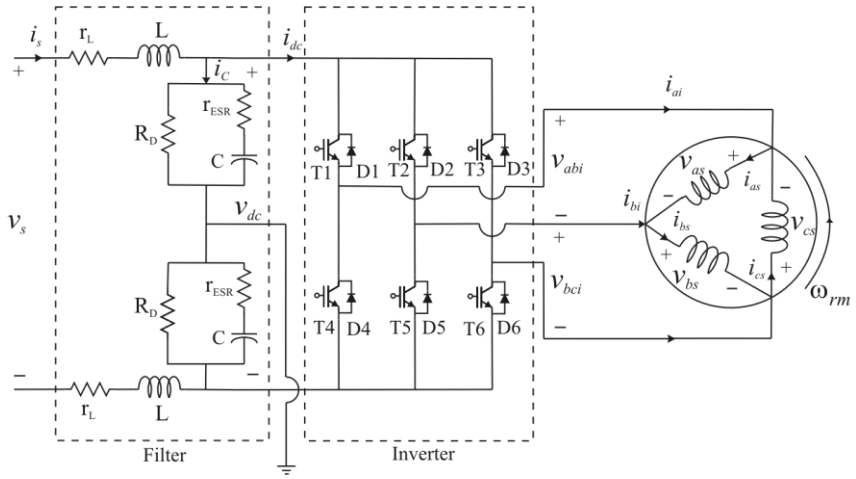

Figure 4 Propulsion drive primary components

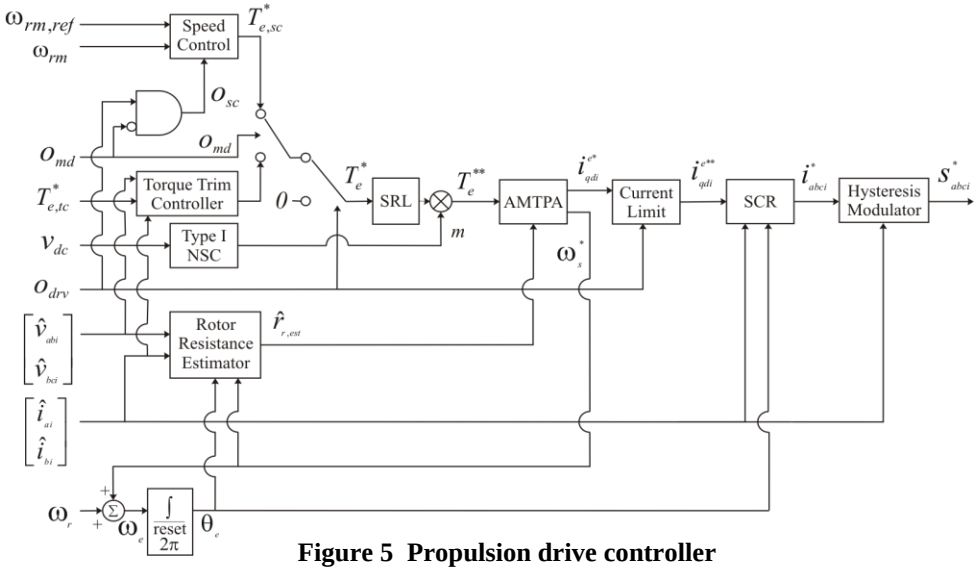

Figure 5 Propulsion drive controller

3. PROPULSION DRIVE MODEL

The SPS ship propulsion system is composed of an input LC filter, PD propulsion drive, controller and induction machine connected to a dynamometer which can emulate 4-quadrant hydrodynamic loads. The primary components are presented in [11]. The input filter has a 1 kHz cut-off. The induction drive is a 4 pole, 460 V, 60 Hz, 50 Hp delta-connected squirrel cage induction machine. The overall control strategy for the propulsion drive is shown in Figure 5. The propulsion controls can operate in either torque or speed command modes and can coordinate with a pulsed load. The controller implements the adaptive maximum torque per amp (AMTPA) control described in [12]. In commanded torque mode, $T^*_{e,tc}$ is processed by the torque trim controller which ensures tracking between the commanded torque and the estimated torque. Torque estimation based on the measured motor current and voltage as well as anti-windup as documented in [11]. The propulsion controller contains a provision to improve stability by modulating the torque command via non-linear stabilizing control (NSC) [13]. This feature is disabled for the studies presented herein. The commanded torque, T^*_e, is slew rate limited and commanded current is limited to protect the inverter. The output of this limiter is processed by the synchronous current regulator described in section 13.11 of [7] and delta-hysteresis modulation controls the inverter.

The detailed waveform SPS model includes all leakages and magnetizing saturation. The simplified waveform model neglects saturation and replaces the AMTPA control with constant slip MTPA control as set forth in section 14.3 of [7]. The primary difference between the detailed waveform model and the detailed non-linear average value model (NLAM) is the use of a synchronous reference frame. The simplified NLAM assumes that the commanded current can be tracked by the inverter removing the current regulator from simulation. Also, a reduced order model for the induction machine is used. Complete models and parameter data can be obtained from the references [11], [14] and website www.usna.edu/ESRDC.

4. STABILITY ANALYSIS

Power electronics based power distribution, being a key technology in electric ships must be robust. A shipboard isolated power system composed of fast power electronics coupled with transient loads and constant power loads of the same order as the generation plant require an additional level of analysis to guarantee that the system does not exhibit unstable operating points. One such approach is that of generalized immittance based stability analysis [15]. This analysis method represents components as generalized immittances (for example impedances or admittances) which bound model behavior in the frequency domain. A significant advantage of this analysis is that it considers entire sets of equilibrium (operating) points at a time, so that a single analysis can be used to explore the stability properties of a system over its entire operating range. Another advantage is the potential to develop *composable* systems such as next generation integrated power systems which guarantee system stability based on component interface specifications.

To illustrate the generalized immittance method [16], consider the simple source-load system of Figure 6. Let the small-signal impedance characteristic of the source at an operating point x be denoted Z_x, and let the small-signal admittance characteristic of the load be denoted Y_x. Let the set Z represent the generalized impedance and the set Y represent the generalized admittance. Thus, $Z_x \in Z$ and $Y_x \in Y$ for all operating points of interest. The variation of values stems both from nonlinearities as well as parameter uncertainties.

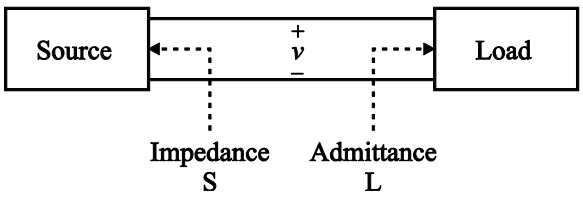

Figure 6 Simple source – load system

The next step is to select a stability criteria with a desired gain margin GM and phase margin PM. Using generalized immittance analysis, specification of a generalized source impedance (or load admittance) constrains the allowable load admittance (or source impedance). The constraint is found such that if the generalized load admittance (or source impedance) does not intersect the forbidden region, then the Nyquist contour of $Z_x Y_x$ will not cross the stability criteria boundary. This in turn ensures that the Nyquist contour of $Z_x Y_x$ cannot encircle –1, which in turn ensures that all operating points considered are locally stable.

The generalized immittance based stability analysis was conducted using the open-source MATLAB-based dc stability toolbox [17] which was developed under prior investigations and remains an active research tool [16]. For the analysis herein, the GS-1 system presented in Figure 3 provides the source impedance model. Likewise, the propulsion system in Figure 4 provides the load admittance model. The gain margin and phase margin values used for this analysis are 6 dB and 30 degrees respectively.

The application of the generalized immittance based stability analysis to the system described in this paper consists of analyzing two cases. The base case will be shown to be stable, and a modified case that will be shown to be unstable. Figure 1 includes the testbed provisions to alternate between the two cases on the fly. The base case is defined by the state of the two switches in the output filter of the generation system and the two switches in the input filter of the propulsion load being in a closed state. This results in an effective capacitance and ESR across the bus of 1.5 mF and 0.0682 Ω for the generation system, and 1.5 mF and 0.1468 Ω for the propulsion load. The modified case only differs from the base case in that all four switches are opened. This removes C_{dc2} and r_{Cdc2} from the generation system, and C and r_{ESR} from the propulsion load. The effective capacitance and ESR become 100 μF and 0.752 Ω, respectively for both the generation system and the propulsion load. This modified case will be shown to be unstable when the propulsion drive is operating at a full load which corresponds to a torque command of 200 Nm at 1500 rpm.

Figure 7 and Figure 8 depict the stability analysis results for the base case and the modified case. Both figures contain a generalized source admittance constraint and generalized load admittance. As can be seen in Figure 7, the stable GS-1 and propulsion load base case contains no intersection between the source constraint and the load admittance. This implies that across the entire frequency range there is an argument for stability.

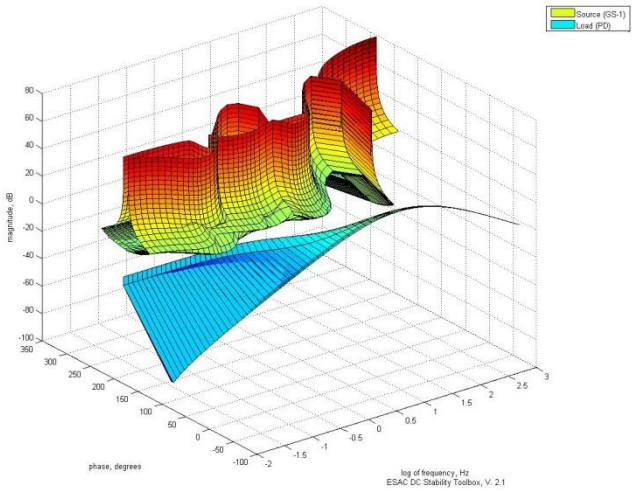

Figure 7 Stable GS-1 and propulsion load case

The Figure 8 modified case distinctly shows an intersection between the source constraint and the load admittance, implying a possible instability at certain operating points. Comparison of experimental stability behavior with time domain simulation studies and generalized immittance analysis is presented in the next section.

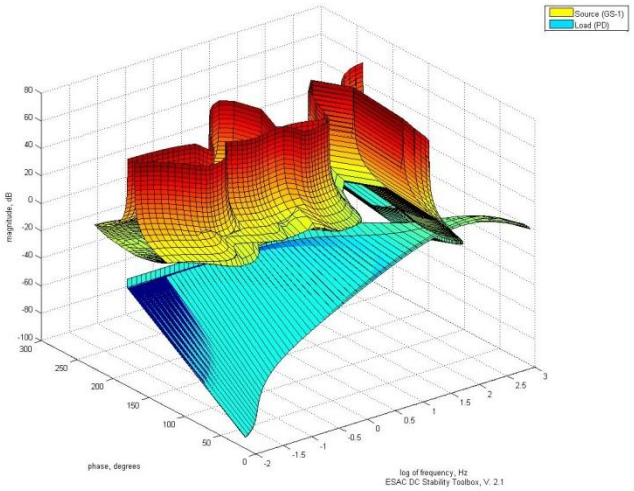

Figure 8 Unstable GS-1 and propulsion load case

5. ACSL SIMULATION AND VALIDATION

The Advanced Continuous Simulation Language (ACSL) is the primary simulation tool used in this investigation. The testbed simulations are numerically stiff and contain many switching states. ACSL has been found to have one of the best solvers for this difficult class of numerical problems. Routines for the complete simulation of the dc testbed have been developed using a modular and systematic approach. Two macro libraries are used in the simulation; the model library and the component library. The model library contains high level modules such as the generator, propulsion drive or induction motor. This library allows the user to easily instantiate various system configurations. The component library contains lower level macro models which encapsulate the details of each component model. Together, various system topologies can be constructed using the concise model library modules while the component library contains the detailed simulation building blocks. Complete models can be obtained from the reference [18] and website www.usna.edu/ESRDC.

5.1. Study 1: Step change in resistive load

In the first validation study, the system is at steady-state with the propulsion motor at half-load condition with T_e = 100 Nm and ω_{rm} = 1500 rpm. At t ≈ 0.20 s, a shunt resistive load of R_{shunt} = 60.2 Ω is added to the system. Figure 9 compares the detailed waveform simulation results and measured testbed data. The experimental data contains higher harmonic content due to high-frequency edge rate noise (in the MHz regime), and significant double-fundamental frequency ripple components associated with imbalances within the ac system. Overall, the correlation is very good.

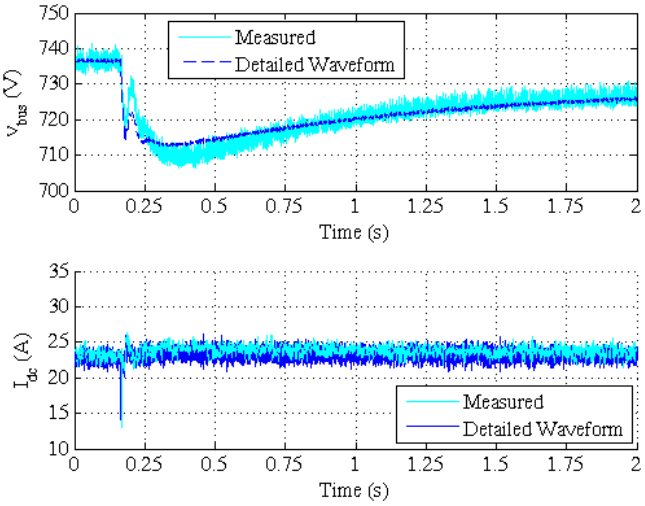

Figure 9 Study 1: Step change in resistive load

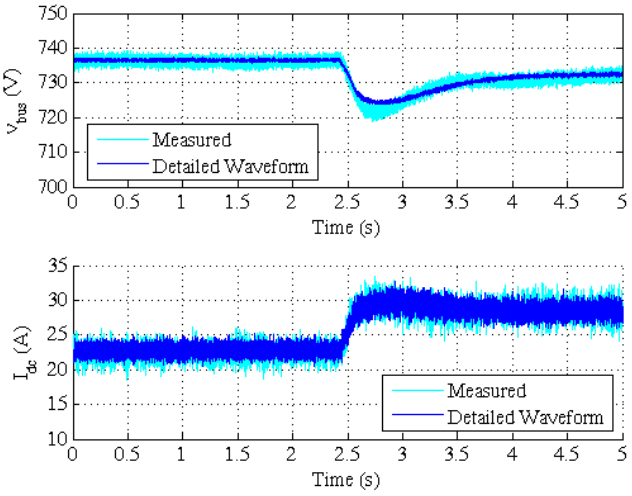

Figure 10 Study 2: Step change in torque command

5.2. Study 2: Step Change in Torque Command

As in the first validation study, the second study begins with the system at steady-state with the propulsion motor at half-load condition with T_e = 100 Nm and ω_{rm} = 1500 rpm. At t ≈ 2.3 s, the commanded torque is stepped up from 100 Nm to 125 Nm while holding the speed constant. Figure 10 compares the detailed waveform simulation results and measured testbed data. Once again the experimental data contains higher harmonic content and overall, the correlation is very good. Figure 11 compares the detailed simulation waveform and measured testbed data under steady state conditions. Note the excellent correlation between the detailed waveform simulation and testbed measurements.

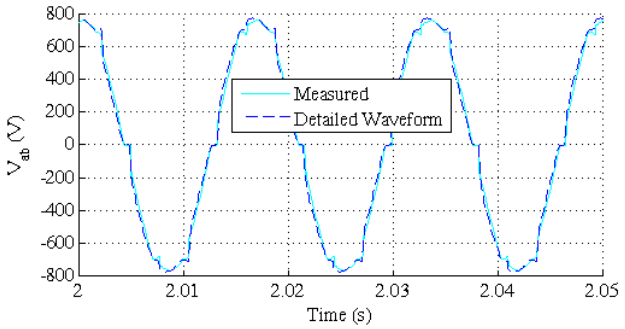

Figure 11 Study 2: Steady state waveform

5.3. Study 3: Change in Bus Capacitance

In the third validation study, the propulsion drive is operating at the 100 Nm half-load condition at 1500 RPM. The input capacitance of propulsion system is reduced from 1.5 mF to 100 uF. In the simulation, this change occurs at $t \approx 5$ s and in the experiment, the change occurs at $t \approx 4.5$ s. Next at $t \approx 11$ s the output capacitance of the generation system is reduced to from 1.5 mF to 100 uF. As seen in, the simulation results closely match the hardware results during this non-linear event.

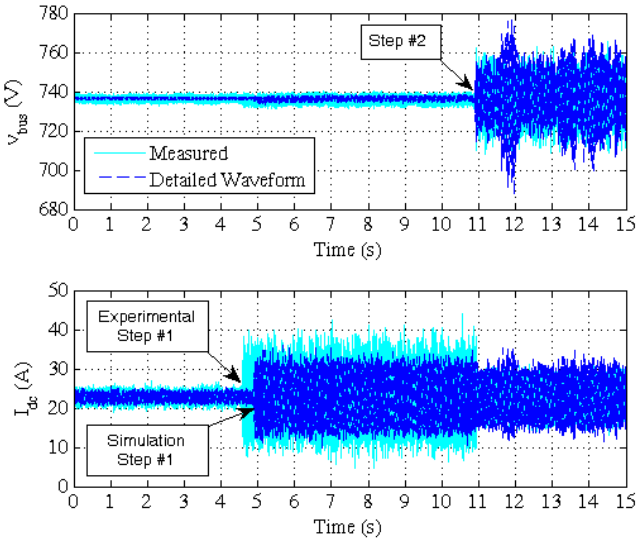

Figure 12 Study 3: Change in bus capacitance

Figure 13 depicts Study 3 (Change in Bus Capacitance) results for a propulsion load torque command of 200 Nm which corresponds to full-load conditions. All other study parameters are the same as in the previously presented Study 3. Instability in physical systems can be seen as either runaway behavior leading to system shutdown or as sustained oscillations not harmonically related to the switching of power semiconductors as mentioned in [18]. As can be seen, once the bus capacitances on both the generator and the propulsion drive are switched out (at $t \approx 13$s), the system exhibits unstable behavior and eventually shuts down in both simulation and hardware. This corresponds to the Section 4 Stability Analysis results obtained using the generalized immittance based stability analysis.

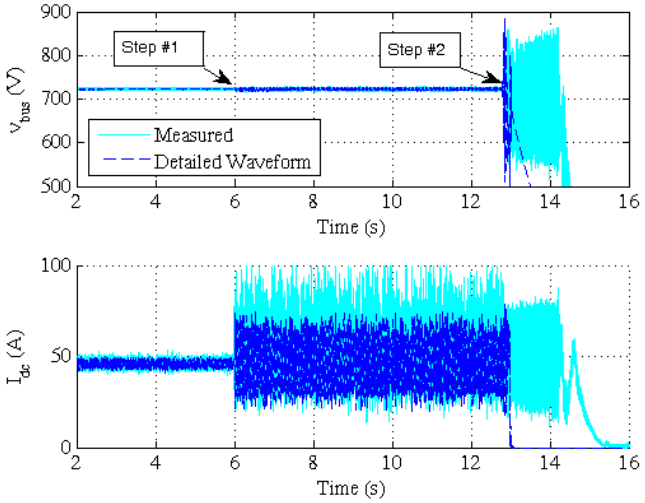

Figure 13 Study 3 at full load depicting instability

6. SIMULINK SIMULATION AND VALIDATION

6.1. Simulink Modeling

In order to provide more readily accessible dc tested simulations which are equivalent to the simplified (conventional) versions of the ACSL truth models, the simplified waveform and AVM models were converted to Simulink. The detailed ACSL waveform and AVM models which include saturation, distributed machine effects and other details were not converted to Simulink.

Most portions of the simplified models can be implemented in Simulink block diagram format in a straightforward manner. However, portions of the models such as complex conditional logic are difficult to model in block diagram format. In these situations, Embedded MATLAB Language subset function blocks are used. The Simulink inputs and outputs correspond to those defined in ACSL models. In the case where ACSL macro inputs are constant parameter values which are not used in other blocks, these parameter values are defined as Simulink parameters with values assigned via Simulink block parameter dialog boxes. Parameters that are inherent to a subsystem are specified in the associated parameters dialog box or the subsystem initialization pane. The initialization pane is more convenient for large numbers of parameters or parameters that are calculated from other parameters. Online help was extracted from the testbed documentation. Simulink memory blocks are used to break algebraic loops and to retain previous values.

6.2. Simulink Simulation Validation

The Simulink dc testbed models were compared with the ACSL standard waveform and AVM time domain simulation results for the three study scenarios presented in the preceding ACSL simulation and validation section. For these test scenarios, the Simulink and ACSL standard waveform and AVM simulations were found to be equivalent. Figure 14 illustrates this correspondence for the study 2 step in commanded torque from 100Nm to 125Nm.

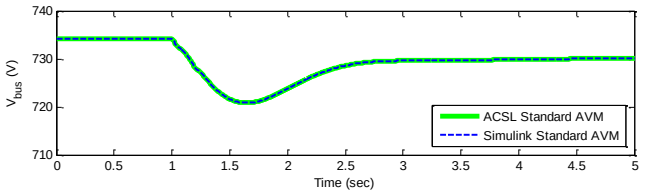

Figure 14 (a) Average value model dc bus voltage

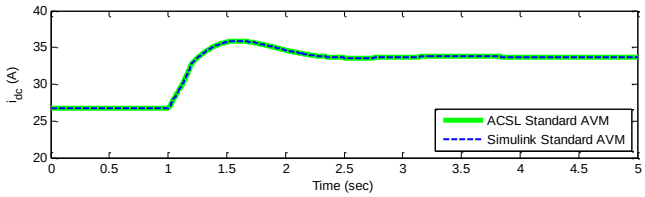

Figure 14 (b) Average value model dc current

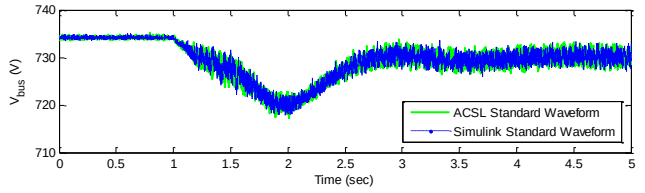

Figure 14 (c) Waveform model dc bus voltage

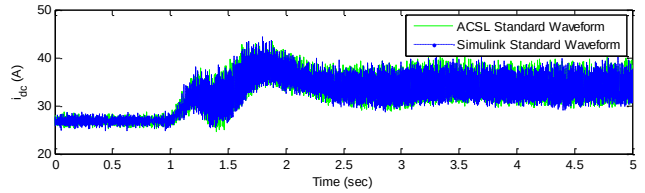

Figure 14 (d) Waveform model dc current

Figure 14 Study 2: ACSL and Simulink Comparison

7. SUMMARY AND CONCLUSIONS

A new medium voltage dc testbed has been established along with first principles state-of-the-art mathematical models. These models were developed with four levels of fidelity: (1) detailed waveform models, (2) detailed average value models, (3) conventional (simplified) waveform models and (4) conventional (simplified) average value models. Key aspects of the testbed and associated models are presented with references to complete simulations, models, parameters and experimental data. All models are available in the ACSL simulation environment and the conventional waveform and average value models are also available in Simulink. The ACSL and Simulink simulation studies are presented and are shown to provide the same results. Successful experimental validation test results of the detailed waveform "truth" models were presented for three test scenarios: (1) step addition of a resistive load, (2) step increase in commanded propulsion motor torque and (3) steady state stability testing at half and full load conditions. As expected, the detailed waveform model simulation results match the experimental results. The less complex models also function has expected. While the close correlation between the various models and testbed experiments establish modeling and simulation credibility, additional investigations continue. In particular, the testbed has higher than expected harmonic content at double-fundamental frequency.

A generalized immittance based stability analysis of the testbed was performed and synopsized. Testbed stability validation experimental results coincide with both the inception of limit cycle oscillation in the time domain simulations and the generalized immittance based stability analysis. The ability to predict and simulate the onset of limit cycle oscillation is a strong result. The results are also consistent with previous testing on the prior naval combat survivability testbed [19]. All of the testbed models, simulations, experimental data and the dc stability toolbox are in the public domain and available for download to other researchers at www.usna.edu/ESRDC.

8. FUTURE WORK

Extending the dc testbed operation and analysis to incorporate the existing second generator, pulsed power load and dc zonal distribution system will provide a richer research ensemble. Efforts are also underway to achieve geographical distributed cosimulation with other institutions. Also, refinements in component parameter measurements, estimation and system response data acquisition continue. Now that the detailed simulation can model the onset of limit instability, efforts are underway to accurately model the shut down process.

Presently, the generalized immittance based stability methods are the most promising design oriented stability tools. Because these methods are *composable* it may be possible to derive practical interface specifications to ensure the stability of next generation integrated power systems. Extensions of this work to achieve an integrated time-domain, frequency-domain, and generalized immittance analysis based design is a high priority.

Presently, work is underway to establish ESRDC baseline simulations of representative ac, higher frequency ac and medium voltage dc next generation integrated powers systems. These simulations will span the electro-mechanical-thermal-fluid-spatial-control system domains to establish integrated models in support of early design space exploration. This work coupled with the design space exploration described in [20] has the highest priority.

ACKNOWLEDGMENT

This work was primarily supported by the Office of Naval Research through the Electric Ship Research and Development Consortium, Office of Naval Research Grants N-00014-08-0080, N-00014-10-WX21446 and N-00014-09-WR20184.

REFERENCES

[1] N.N. Schulz et al., "The U.S. ESRDC advances power system research for shipboard systems," in *43rd International Universities Power Engineering Conference, UPEC 2008*, Padov, Italty, 2008, pp. 1-4.

[2] M. Bash et al., "A Medium Voltage DC Testbed for Ship Power System Research," in *IEEE Electric Ship Technologies Symposium, ESTS 2009*, Baltimore, 2009, pp. 560-567.

[3] S.D. Pekarek, B.T. Kuhn, S.F. Glover, J. Sauer, D.E. S.D. Sudhoff, "Naval Combat Survivability Testbeds for Investigation of Issues," in *Proc. of the IEEE Power Engineering Society Summer Meeting*, Chicago, 2002, pp. 347 - 350.

[4] J.M. Crider and S.D. Sudhoff, "Reducing Impact of Pulsed Power Loads on Microgrid Power Systems," *IEEE Transactions on Smart Grid*, vol. 1, no. 3, pp. 270-277, December 2010.

[5] D.C. Aliprantis, S.D. Sudhoff, and B.T. Kuhn, "A synchronous machine model with saturation and arbitrary rotor network representation," *IEEE Transactions on Energy Conversion*, vol. 20, pp. 584-594, September 2005.

[6] D.C. Aliprantis, S.D. Sudhoff, and B.T. Kuhn, "A brushless exciter model incorporating multiple rectifier modes and Preisach's hysteresis theory," *IEEE Transactions on Energy Conversion*, vol. 21, no. 1, pp. 136-147, March 2006.

[7] P.C. Krause, O. Wasynczuk, and S.D. and Sudhoff, *Analysis of Electric Machinery and Drive Systems, 2nd Edition*. New York, USA: John Wiley and Sons/IEEE Press, 2002.

[8] S. D. Sudhoff, K.A. Corzine, H.J. Hegner, and and D.E. Delisle, "Transient and Dynamic Average-Value Modeling of Synchronous Machine Fed Load-Commutated Converters," *IEEE Tranaction on Energy Conversion*, vol. 11, no. 3, pp. 508-514, September 1996.

[9] A.M Cramer et al., "Modeling and Simulation of an Electric Warship Integrated Engineering Plant," in *Proceedings of the 2006 SAE Power Systems Conference*, New Orleans, 2006, pp. 1-23.

[10] M. Bash and R.R. Chan, "Medium Voltage DC Testbed: Generator System GS-1," Purdue University, West Lafayette, IN, Model Documentation and Reports.zip (3.1MB) 8/13/2010 http://www.usna.edu/ESRDC, 2010.

[11] C. Harianto, "Medium Voltage DC Testbed: Propulsion Drive," Purdue University, West Lafayette, IN, Model Documentation and Reports.zip (3.1MB) 8/13/2010 http://www.usna.edu/ESRDC, 2009.

[12] C. Kwon and S.D. Sudhoff, "An improved maximum torque per amp control strategy for induction machine drives," in *Twentieth Annual IEEE APEC 2005*, Austin, 2005, pp. 740 - 745.

[13] S.F. Glover and S. D. Sudhoff, "An Experimentally Validated Nonlinear Stabilizing Control for Power Electronics Based Power Systems," *SAE Transactions, Journal of Aerospace*, vol. 1, no. 10.4271/981255 , pp. 68-77, April 1998.

[14] University Purdue, "ACSL detailed and simplified waveform and average value models," Purdue University, West Lafayette, IN, ACSL Models.zip (539.3kB) 12/29/2009 15:37 www.usna.edu/ESRDC, 2010.

[15] S.D. Sudhoff, S.F. Glover, P.T. Lamm, D.H. Schmucker, and D.E. Delisle, "Admittance space stability analysis of power electronic systems," *Aerospace and Electronic Systems, IEEE Transactions on*, vol. 36, no. 3, pp. 965-973, July 2000.

[16] S. Sudhoff and M. Crider, "Advancements in Generalized Immittance Based Stability Analysis of DC Power Electronics Based Distribution Systems," in *IEEE Electric Ship Technologies Symposium, ESTS 2011*, Alexandra, VA, 2011, pp. 1-6.

[17] S. D. Sudhoff, "DC Stabilty Toolbox 3.0," Purdue University, West Layfatte, IN, source code aand manual https://engineering.purdue.edu/ECE/Research/Areas/PEDS, 2010.

[18] Y. Lee, "Simulink dc testbed simplified waveform & average value models ," U. S. Naval Academy, Annapolis, MD, Simulink Models.zip (2.0MB) 12/29/2009 15:37 www.usna.edu/ESRDC, 2010.

[19] S.D. Sudhoff et al., "Stability analysis methodologies for dc power distribution systems," in *Proceedings of the 13th International Ship Control Systems Symposium*, Orlando, 2003, p. Paper 235.

[20] A.M. Cramer, E L. Zivi, and S.D. Sudhoff, "Modeling and Simulation of an Electric Warship Integrated Engineering Plant for Battle Damage Response," in *submitted to Modeling and Simulation – Methodology, Tools, Applications (M&S-MTA'11)*, The Hague, 2011, pp. 1-7.